Available online at www.sciencedirect.com

ScienceDirect

Current Opinion in Structural Biology

Machine learning across label-free optical measurement platforms for cellular dynamics and biomechanics

Balint Beres[1,2] and Robert Horvath[1,3]

Label-free optical biosensing combined with machine learning enables live-cell analysis with high spatial and temporal resolution and can improve cell-state classification, response profiling, and estimation of biomechanically relevant variables. This review organizes works into single-modal and multimodal workflows. In single-modal analysis, representation-oriented approaches improve signal quality and provide data reconstruction or calibration before modeling, whereas inference-oriented approaches map optical data to phenotypes, adhesion behavior, or other biologically relevant variables. These roles are examined across surface-enhanced Raman spectroscopy (SERS), surface plasmon resonance/resonant waveguide grating (SPR/RWG), and digital holographic microscopy (DHM). Multimodal workflows are grouped into reference-based calibration, in which an auxiliary modality supervises a primary platform, and joint multimodal inference, in which complementary readouts are fused to estimate cell state robustly.

Addresses
[1] Nanobiosensorics Laboratory, Institute of Engineering Physics and Materials Science of the HUN-REN Energy Research Centre, Konkoly-Thege Miklós út 29-33, Budapest H-1121, Hungary
[2] Department of Automation and Applied Informatics, Faculty of Electrical Engineering and Informatics, Budapest University of Technology and Economics, Műegyetem Rkp. 3., 1111 Budapest, Hungary
[3] Institute of Biophysics, HUN-REN Biological Research Centre, Temesvári Krt. 74., 6726 Szeged, Hungary

Corresponding author: Horvath, Robert (horvath.robert@ek.hun-ren.hu)

Current Opinion in Structural Biology 2026, **101**:103352

This review comes from a themed issue on **Single Cell and Cell Cell Interactions (2026)**

Edited by **Sandor Kasas** and **Giovanni Longo**

For a complete overview see the Issue and the Editorial

Available online

https://doi.org/10.1016/j.sbi.2026.103352

Introduction

Live-cell biomechanics includes several dynamic processes such as adhesion, detachment, migration, and mechanically coupled biochemical remodeling. These can be captured using label-free optical systems, which share the same operating principle: a biological process perturbs an optical field, which the instrument changes into a measurable signal. This distinction is essential because label-free optical platforms differ in the produced modality. Surface-enhanced Raman spectroscopy (SERS) captures chemically rich spectra [1], whilst surface plasmon resonance (SPR) and other surface-bound optical mode systems measure refractive-index-dependent resonance signals [2,3]. Resonant waveguide-grating (RWG) captures dynamic mass redistribution and near-surface adhesion kinetics [4–6], and digital holographic microscopy (DHM) reconstructs phase and morphology from holographic interferograms [7,8]. Machine learning-based methods are used either to stabilize the captured signal or to convert it to biologically or biomechanically informative outputs.

This review uses a modality-based structure to discuss ML integrations in label-free molecular and cellular sensing. Applications are grouped into three single-modal categories: *(i)* spectral measurements, *(ii)* evanescent-field refractometric sensing for interfacial kinetics, and *(iii)* image- or video-based phase microscopy. ML roles are divided into representation-oriented and inference-oriented integrations.

Representation-oriented ML performs signal conditioning for better reliability, comparability, or physical interpretability of the optical signal before decision modelling. In SERS, this includes spectral conditioning, denoising, cross-device standardization, and spectral fusion [9–12]. In SPR and plasmonic refractometric sensing, it includes full-spectrum refractive-index regression, recovery of surface refractive-index

dynamics, and surface or coating-property modelling [13–16]. In RWG and guided-mode resonant sensing, it includes drift handling, spatial response extraction, and image-guided attribution of single-cell adhesion-contact signals [17]. In DHM, ML supports deep-learning-based phase processing and hologram reconstruction workflows [7,8,18–22]. In these workflows, data separation steps, such as threshold selection, remain an important source of variability. In SERS/Raman pipelines, thresholds define which weak peaks, low-SNR spectra, or outlier spectra are rejected, and therefore influence the chemical information passed to denoising, calibration, or classification models [23,24]. In SPR and RWG workflows, thresholds enter drift correction, refractive-index recovery, limit-of-detection estimation, contact-map construction, and acceptance of wavelength-shift or sensorgram traces [25]. In DHM and quantitative phase imaging, thresholds affect Fourier-domain filtering, phase-map acceptance, cell/background segmentation, and reconstructed feature extraction; automatic histogram-optimized procedures can reduce manual bias but still require validation against controls or ground truth [26,27]. Thresholds should therefore be reported as integral preprocessing parameters, tied where possible to instrument noise, calibration standards, or physically meaningful signal-to-noise criteria and tested by sensitivity analysis. This is especially important when downstream inference models are trained on thresholded representations, because threshold choices can strongly influence estimated feature distributions or biophysical-parameter distributions of samples.

Inference-oriented ML transforms measured or reconstructed data into biologically or biomechanically interpretable outputs. In SERS, this includes intracellular stress readouts [9], metabolite-gradient inference around living cells [28], and SERS nanoendoscopy or optophysiology for cell-proximal biochemical sensing [29]. In SPR and related plasmonic refractometric sensing, inference mainly concerns biomolecular binding, receptor interaction, biomarker response, and sensorgram-pattern interpretation [2,3]. In RWG, ML is applied for time-series and spatial adhesion-kinetic single-cell classification [17,30] and, when paired with direct force references, calibration of adhesion-force variables [31]. In DHM, inference-oriented ML uses phase maps, masks, morphology time series, and trajectories for microbial tracking, flow-cytometry classification, and mechanism-of-action inference [32–35].

The following sections discuss spectral, refractometric, and image- or video-based workflows along these two ML roles. The final section considers multimodal workflows grouped into two categories. In reference-based calibration, reference domains, fluorescence labels, or direct force measurements are used to calibrate or supervise the interpretation of a primary label-free signal [11,17,31,36]. In joint multimodal inference, complementary measurements are fused to estimate mechanochemical or biomechanically relevant cell states more robustly than any single readout alone [28,29,31,34,37,38]. Figure 1 summarizes this framework, and Table 1 compares the corresponding representation- and inference-oriented ML roles.

Single-modal workflows

Single-modal workflows are defined as experimental designs in which one optical platform supplies the primary data stream and the ML model is constrained by that platform's native observable. In the following three subsections, ML integrations in label-free optical systems are discussed using three modality-based categories: spectral, refractometric sensing for interfacial kinetics, and image- or video-based phase microscopy.

Spectral methods

Spectral sensing methods are represented here by SERS-based systems, because SERS supplies the chemical layer of label-free cellular analysis. Early silver-electrode studies established that Raman scattering from surface-bound molecules can be enhanced, enabling weak molecular fingerprints to be detected from small amounts of material [40,41]. In modern biosensing, this enhancement allows SERS to probe metabolites, intracellular chemical state, and cell-proximal biochemical gradients relevant to cellular dynamics [1,28,29,42]. For biomechanical phenotyping, SERS reports the biochemical context in which adhesion, stress response, and drug-induced remodeling occur, but SERS-derived features should remain interpreted as metabolic or chemical descriptors unless calibrated against mechanical variables. The traditional analysis methods of SERS/Raman data are built around chemically assigned bands, peak intensities or peak ratios, baseline correction, dimensionality reduction, and chemometric calibration. Methods such as PCA, PCA-DA, PLSR, and conventional spectral preprocessing remain important because they preserve a direct connection between the measured spectrum and molecular interpretation. ML-based processing extends this framework since SERS spectra are high-dimensional and variable: hot-spot geometry, substrate heterogeneity, molecular adsorption, matrix background, baseline drift, and device-dependent shifts can alter the measured fingerprint before biological interpretation [1,42–44].

Representation-oriented SERS applications include denoising, baseline correction, and multi-acquisition enrichment. Zaki et al. developed an explainable SERS bioquantification framework in which synthetically contaminated spectra are denoised before quantitative prediction [10]. Mahmud et al. addressed cross-device variability by mapping portable-instrument spectra toward a laboratory-grade reference domain before bacterial recognition [11]. Wang et al. used dual-wavelength

Figure 1

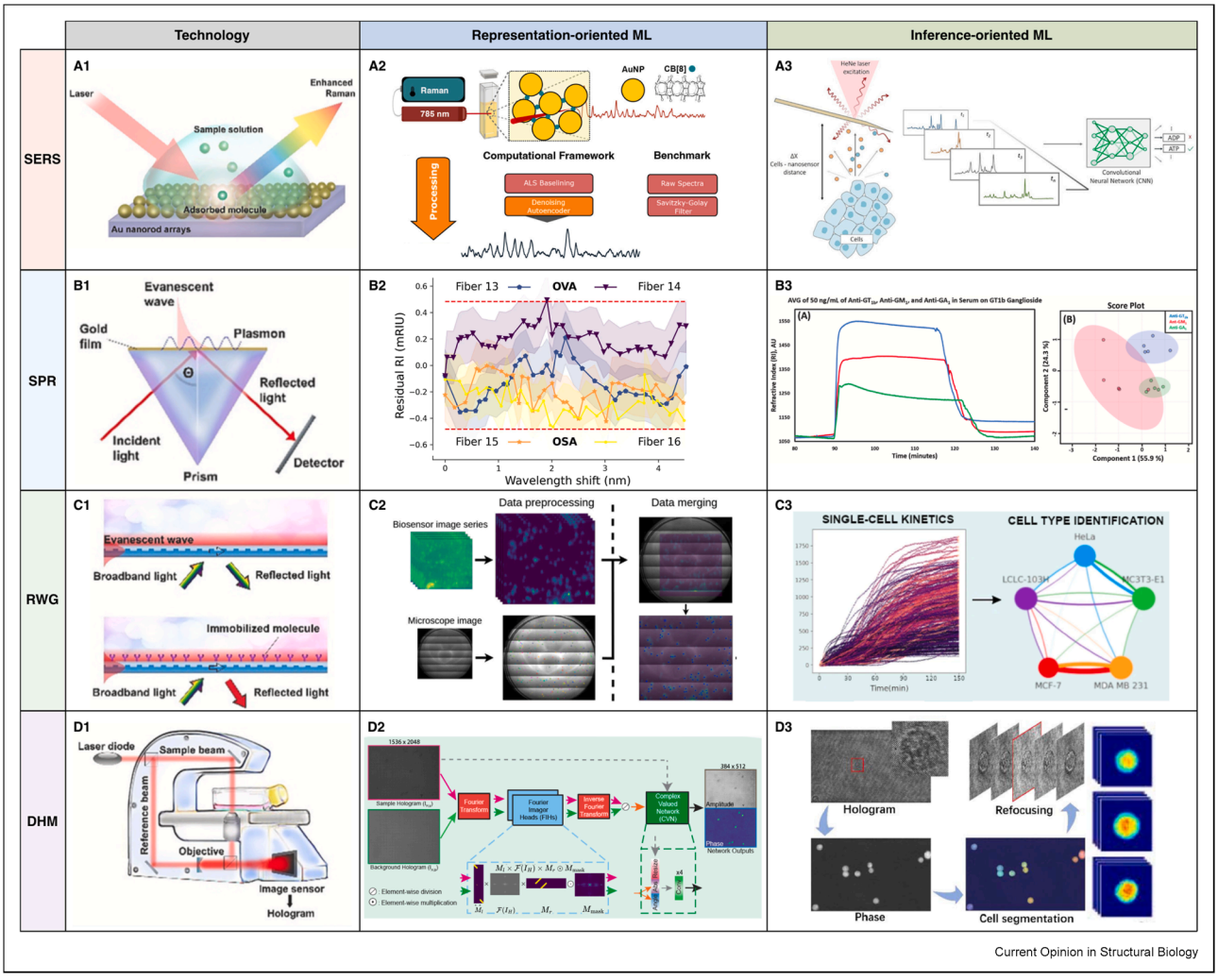

Single-modal representation- and inference-oriented ML across label-free optical sensing technologies. Rows correspond to SERS, SPR, RWG, and DHM. The first column, A1-D1, illustrates the underlying sensing technology [6]. The second column shows representation-oriented ML, where the measured signal is denoised, standardized, reconstructed, or converted into a more physically interpretable representation before biological inference. These include A2, SERS signal denoising [11], B2, SPR/plasmonic refractometric readout recovery [14], C2, RWG image-guided single-cell signal extraction [17], and D2, DHM hologram reconstruction [8]. The third column shows inference-oriented ML, where measured or reconstructed representations are mapped to biological or cellular outputs. These include A3, SERS biochemical-state inference [28], B3, SPRi biomarker-pattern inference [39], C3, RWG adhesion-kinetic cell-type identification [30], and D3, DHM/holographic-flow-cytometry cell discrimination [34]. Panels are adapted from the cited works.

and multisubstrate fusion to construct higher-dimensional SERS fingerprints [12]. Chen et al. combine SERS nanoprobes with a feature extractor neural network and a 1D-CNN quantification model to detect intracellular reactive oxygen species [9]. The study is notable because the learned representation is tied to chemically specific SERS features rather than treated as a generic classifier output. Taken together, these studies show that representation-oriented ML in SERS is not only about reducing measurement device-related artifacts, but about preserving chemically relevant structure while making spectra comparable across instruments and acquisition conditions.

Inference-oriented SERS models convert spectral fingerprints into biochemical outputs through classification, regression, or latent representation learning. Lussier et al. combined SERS nanoprobes with ML-driven optophysiology to resolve multiplexed metabolite gradients near living cells, producing a local

Table 1

Label-free optical sensing technologies and their representation- and inference-oriented ML roles.

Technology/ workflow	Primary readout	Data object	Representation-oriented ML	Inference-oriented ML	Biomechanical role	Refs
SERS/Raman	Raman/SERS molecular fingerprints.	High-dimensional spectra.	Denoising; baseline correction; device transfer; fusion.	Metabolic/stress inference; metabolite gradients.	Indirect mechanometabolic context.	[1,9–12,28,29,40–44,54]
SPR/plasmonic RI	Near-surface RI and resonance kinetics.	Spectra; sensorgrams; RI traces.	Full-spectrum RI recovery; drift correction.	Binding, biomarker, or assay-response inference.	Interfacial biochemical dynamics.	[2,3,5,13–16,25,39,55]
RWG/guided-mode	Adhesion/contact kinetics; DMR.	Time traces; contact maps.	ROI extraction; contact-map construction; normalization.	Cell typing; adhesion/drug-response phenotyping.	Strongest single-modal adhesion readout.	[4–6,17,25,30,31,45–47]
DHM	Phase-derived morphology and motion.	Holograms; phase maps; trajectories.	Phase reconstruction; aberration/refocus correction.	Tracking; flow cytometry; MoA and morphodynamic inference.	Whole-cell morphodynamics; mechanics only with labels.	[7,8,18–22,26,32–38,50,53,56–59]

The table summarizes primary readouts, data objects, ML functions, biomechanical relevance, and supporting references for SERS/Raman, SPR, RWG, and DHM workflows.

biochemical-state readout rather than only a diagnostic class [28]. Chisanga et al. further positioned ML-driven SERS nanoendoscopy and optophysiology as routes toward intracellular, extracellular, and in vivo chemical measurements from complex vibrational spectral datasets [29]. These studies make SERS relevant to mechanobiology when biochemical dynamics are interpreted together with adhesion, morphology, or mechanical references.

Evanescent-field refractometric sensing for interfacial kinetics

Surface-integrating optical platforms examine the thin near-surface region where adsorption, cell attachment, adhesion, detachment, and cell—substrate interactions take place. This approach is heavily applied to adhesion-centered cellular dynamics and biomechanically relevant surface phenotypes modelling. SPR and RWG provide broad examples for representation-oriented and inference-oriented analysis. SPR and related plasmonic platforms convert near-surface refractive-index changes into resonance shifts, spectra, or kinetic sensorgrams, while RWG and guided-mode resonant systems extend near-surface optical sensitivity toward live-cell adhesion, spreading, receptor-mediated signaling, and dynamic mass redistribution with increased throughput [2—5,25,45]. Standard quantitative methods for SPR and guided-mode systems are based on physically interpretable optical and kinetic descriptors. In SPR-type assays, these include resonance-wavelength or resonance-angle shifts, fixed-wavelength intensity changes, refractive-index calibration, sensorgram shape, and Langmuir-type binding models when molecular interaction kinetics are studied [2,3,13,14,25]. In RWG and cellular guided-mode sensing, conventional descriptors include maximum wavelength shift, wavelength-shift rate, integrated wavelength shift, final adhesion level, contact area, and fitted adhesion-kinetic parameters. When paired force measurements are available, robotic fluidic force microscopy (FluidFM)-derived adhesion force and adhesion energy provide direct mechanical reference variables for interpreting optical adhesion signals [31,45—48].

For SPR and plasmonic refractometric sensing, the goal of representation-oriented tasks is to recover a stable physical readout from complex optical responses. Aalizadeh et al. demonstrated this principle using full-spectrum ML modelling for refractive-index sensing, where principal components from entire spectra were used instead of a single manually selected resonance feature [13]. This is a strong example because it suggests that physically relevant sensing information is distributed across the entire spectral response and can be recovered more faithfully by learned models than by peak-tracking heuristics alone. Fasseaux et al. similarly used ML to recover surface refractive-index dynamics

Figure 2

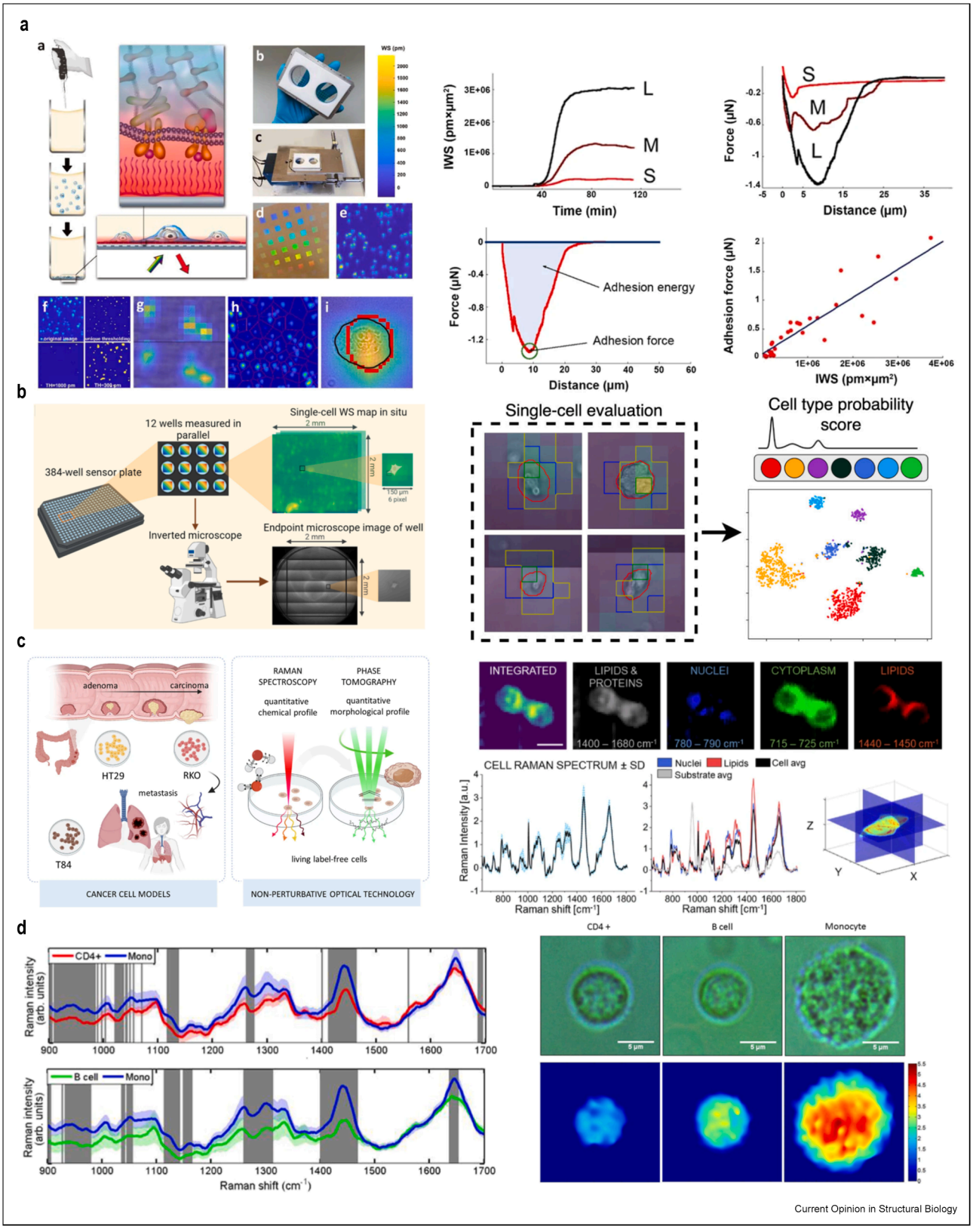

Reference-based calibration and joint multimodal inference workflows for label-free cellular analysis. Panels A and B illustrate reference-based calibration workflows, whereas panels C and D illustrate joint multimodal inference. **(a)** RWG plus robotic FluidFM: label-free optical adhesion kinetics are

from complex spectra, converting them into a physically interpretable surface variable [14]. Single-cell RWG platforms transform raw sensor response into reproducible contact maps or single-cell descriptors before adhesion kinetics can be interpreted biologically, which requires drift handling, extraction of spatially localized signals, and correction for baseline and coating-dependent variation [15–17].

Inference-oriented ML uses SPR- and RWG-based systems to infer biological behavior from near-surface dynamics. In SPR, this is most established for biomolecular binding, receptor interaction, biomarker sensing, and kinetic response analysis, where ML supports classification, regression, or response-pattern interpretation from sensorgrams and spectral responses [2,3]. Single-cell RWG provides living-cell mass redistribution and adhesion-centered phenotyping [4,5]. High-resolution optical adhesion-kinetic data enabled label-free single-cell cancer classification [30], and phase-contrast-assisted RWG adhesion-contact recording enabled activity-based cell-type classification from the spatial distribution of adhesion kinetics [17]. Here, auxiliary imaging defines cell boundaries before classification, tying the learned output to spatially localized adhesion behavior rather than to a bulk-averaged trace alone. The platform was also used to monitor adhesion kinetics during evaluation of anticancer potential and selectivity of natural compounds, supporting models for compound-response classification and selectivity prediction [49].

These studies also show that mechanical references matter for interpreting refractometric signals. FluidFM force measurements have also been integrated with single-cell optical experiments and enable population-level characterization of adhesion parameters [45,46]. Ungai-Salánki et al. linked adhesion-strength and contact-density drops in mitotic cells to label-free optical biosensing, and Sztilkovics et al. combined RWG optical biosensing with robotic FluidFM to monitor adhesion-force kinetics of living cancer cells [31,47]. These studies capture paired datasets in which optical adhesion signals can be calibrated against a mechanically meaningful reference domain. Together, they provide the basis for relating RWG-type optical readouts to adhesion force and for estimating biomechanical variables from refractometric adhesion-kinetic signals [45].

Image-based platforms

DHM illustrates image- and video-based label-free analysis, where acquired holograms must be computationally transformed before biological interpretation. Digital off-axis holography, formalized by Cuche et al., provides access to phase, optical path length, volume, morphology, and trajectories [26]. Recent reviews show that DHM has become a computational imaging field in which ML is used both to reconstruct phase representations and to infer biological states [7,18,22]. These outputs indirectly describe cellular dynamics such as morphology, motility, growth, invasion, and population behavior. Classical DHM and time-lapse image analysis rely on optical phase reconstruction, morphology descriptors, and mathematical descriptions of cell motion. Relevant descriptors include cell area, optical path length, phase volume, dry-mass-related quantities, centroid displacement, speed, turning angle, directional persistence, mean-squared displacement, trajectory confinement, and persistent-random-walk or anomalous–diffusion parameters [26,32,35,50–52]. These quantities provide an interpretable analytical layer between raw holograms or phase maps and higher-level biological conclusions. ML-based reconstruction, segmentation, tracking, and classification can therefore be framed as extensions of established phase-imaging and motility-analysis workflows rather than as replacements for them.

Representation-oriented ML is embedded in the DHM pipeline because the raw hologram is not yet the final biological representation. ML is used for hologram reconstruction, phase retrieval, aberration correction, super-resolution, and robustness to acquisition shifts [7,8,18–22]. Liu et al. introduced OAH-Net for efficient, physics-guided off-axis DHM reconstruction [8]. Bujagouni and Pradhan addressed out-of-distribution failure in deep-learning-based off-axis DHM, while Lin et al. and Galande et al. developed methods for phase-distortion compensation and physics-aware lensless holographic reconstruction [19–21]. Galande et al. also show that deep reconstruction can remain constrained by the imaging model rather than operating as a purely black-box enhancer [21]. Across these studies, the common output is a corrected phase, amplitude, or image representation that can then support later biological analysis.

paired with direct single-cell force measurements, enabling calibration of RWG-derived adhesion signals against adhesion force and adhesion energy [31]. **(b)** Single-cell RWG plus phase-contrast microscopy: phase-contrast images provide cell localization and boundary selection, while RWG records adhesion-contact kinetics; the combined representation is then used for single-cell cancer classification [17]. **(c)** Raman spectroscopy plus phase tomography: Raman spectra provide molecular fingerprints and phase tomography provides morphophysical cell structure, allowing label-free morpho-molecular phenotyping of living cancer cells [54]. **(d)** Raman spectroscopy plus digital holographic microscopy: Raman spectra provide molecular fingerprints and DHM provides quantitative phase-derived morphology, enabling multimodal discrimination of immune-cell populations such as CD4+ T cells, B cells, and monocytes [36]. Panels are adapted from cited works.

Inference-oriented DHM uses reconstructed phase maps, masks, morphology time series, and trajectories to extract biological meaning from image-derived dynamics. Matthews et al. used DHM and deep learning for real-time three-dimensional microbial tracking [32]. Ciaparrone et al. combined holographic flow cytometry with classification for label-free cell discrimination [33]. Sedaghat et al. developed HoloMoA for antimicrobial mechanism-of-action inference and novelty detection [53]. Additional DHM/Holomonitor studies extend this scope to cancer-cell invasion and adhesion-associated morphodynamics [35]. Here, machine learning applications provide both image reconstruction and phase behavior translation into task-specific biological interpretations such as tracking, classification, response profiling, or invasion-related dynamics.

Directions for multimodal integration

Multimodal workflows address the main limitation of single-modal label-free analysis: no individual optical readout captures the full biochemical, adhesive, morphodynamic, and mechanical state of a living cell. In this review, two multimodal roles are separated: reference-based calibration, which uses auxiliary modalities to calibrate or supervise a primary label-free signal, and joint multimodal inference, which combines complementary measurements to infer biological or biomechanical states more robustly. The distinction is useful because some multimodal studies rely on the second modality mainly as a training or calibration reference, whereas others treat both modalities as biologically informative views that should be interpreted together.

Reference-based calibration includes phase-contrast-guided extraction of single-cell RWG adhesion signals, where imaging defines cell boundaries and RWG supplies adhesion-contact kinetics [17], single-cell RWG-FluidFM pairing [31], cross-device SERS standardization [11], and fluorescence-supervised cross-modal learning for label-free DHM-based virtual staining and viability analysis [38], where the fluorescent channel provides a supervision signal that teaches the holographic model a biologically organized representation for segmentation and viability inference. In each case, the auxiliary measurement anchors the interpretation of the primary label-free readout. These are illustrated in Figure 2a, b. Reference-based calibration is therefore best understood as a way to constrain label-free inference with an external modality whose biological semantics are clearer than those of the primary signal alone.

Joint multimodal inference links complementary biological views rather than only calibrating one readout against another. Raman spectroscopy can report molecular fingerprints, whereas DHM and phase tomography can report complementary phase-derived morphology, structure, and dynamic phenotype information [28,29,36,54]. Raman was paired with phase tomography for label-free living-cell phenotyping [54], and with digital holographic phase signatures for discrimination of immune-cell populations such as CD4+ T cells, B cells, and monocytes [36]. The study by Bresci et al. is particularly important because it treats molecular and structural information as co-equal contributors to the final phenotype rather than as helper signals for one another [54]. McReynolds et al. provide an earlier proof that Raman and holographic signatures can jointly improve immune-cell discrimination [36]. Figure 2c, d illustrate these complementary molecular and morphodynamic readouts. More broadly, multimodal fusion is most valuable when the paired modalities resolve different biological axes that would remain ambiguous if interpreted separately.

Conclusions and outlook

ML for label-free optical analysis of cellular dynamics and biomechanical phenotypes is best described as a measurement-to-inference hierarchy. Spectral SERS/Raman methods provide biochemical context [1,9–12,28,29,40–44]; evanescent-field refractometric methods provide adhesion-centered dynamics [2–5,13,14,17,30,31,35,45,47,49,55]; and DHM provides phase-derived morphology, motion and growth descriptors [7,8,18–22,26,32,33,35,50,53]. Within these single-modal workflows, representation-oriented ML stabilizes, reconstructs, or standardizes the primary signal, while inference-oriented ML maps it to cell states, drug responses, or biomechanically relevant phenotypes. Multimodal workflows extend this hierarchy through reference-based calibration and joint multimodal inference to improve accuracy of dedicated modalities or combine information from multiple platform readouts [11,17,28,29,31,33,34,36,38,54].

Looking ahead, progress will depend not only on more capable ML models but also on better paired multimodal datasets, stronger calibration strategies, and clearer links between optical proxies and direct biomechanical references [36–38,45,56–59]. Reliable adoption of these methodologies requires interpretability, standardization, and experimentally grounded validation. For optical sensor data processing pipelines, interpretability or explainability should be treated as part of experimental validation and as an important focus during model development [60–63]. This requires direct links from model behavior to experimentally meaningful observables: Raman/SERS bands or biochemical contexts, refractive-index and adhesion-kinetic features, DHM-derived phase, morphology or trajectory descriptors [10,17,26,50–53]. The main challenge here is that these observables may not reflect underlying biological processes alone. Instrument configuration, substrate chemistry, culture conditions, cell-line history and the different data processing steps can all introduce domain shifts. A second challenge is faithfulness or whether the models

accurately reflect underlying processes: saliency maps, latent variables or reconstructed images may appear biologically plausible while reflecting acquisition artefacts, batch effects or unsupported model extrapolation [60,62]. Practical adoption therefore requires metadata-rich datasets, external and batch-independent validation, uncertainty or reliability estimates, and comparison with orthogonal assays or classical descriptors of morphology, motility, adhesion, and mechanics [61,62]. In this sense, interpretability is successful when ML outputs become experimentally testable biological hypotheses, not merely high-accuracy classifications. Table 1 provides a concise platform-by-platform comparison of the roles discussed here.

Declaration of competing interest

The authors declare that they have no known competing financial interests or personal relationships that could have appeared to influence the work reported in this paper.

Acknowledgments

This research was funded by the Hungarian Academy of Sciences LP2025-15/2025 MTA–HUN- REN EK Lendület "Momentum" Nanobiosensorics Research Group. Project no. [ADVANCED 153121, 2024-1.2.10-TÉT-IPARI-IL-2024-00030] has been implemented with the support provided by the Ministry of Culture and Innovation of Hungary from the National Research, Development and Innovation Fund, financed under the [OTKA, TÉT] funding scheme. Project no. [TKP2021-EGA-04] has been implemented with the support provided by the Ministry of Culture and Innovation of Hungary from the National Research, Development and Innovation Fund, financed under the [TKP2021-EGA] funding scheme.

Data availability

Data will be made available on request.

References

Papers of particular interest, published within the period of review, have been highlighted as:

* of special interest
** of outstanding interest

1. Cialla-May D, Bonifacio A, Markin A, Markina N, Fornasaro S, Dwivedi A, *et al.*: **Recent advances of surface enhanced Raman spectroscopy (SERS) in optical biosensing**. *TrAC, Trends Anal Chem* 2024, **181**, 117990.

2. Butt MA: **Surface plasmon resonance-based biodetection systems: principles, progress and Applications-A comprehensive review**. *Biosensors (Basel)* 2025, **15**:35.

3. Chirco A, Meacci E, Margheri G: **A tutorial review on surface plasmon resonance biosensors: applications in biomedicine**. *ACS Bio & Med Chem Au* 2025, **5**:922–946.

4. Fang Y, Ferrie AM, Fontaine NH, Mauro J, Balakrishnan J: **Resonant waveguide grating biosensor for living cell sensing**. *Biophys J* 2006, **91**:1925–1940.

5. Sahoo PK, Bhat AA, Singh M, Li K: **Recent advances of guided mode resonant sensors applied to cancer biomarker detection**. *Photonics* 2025, **12**:424.

6. Szittner Z, Péter B, Kurunczi S, Székács I, Horvath R: **Functional blood cell analysis by label-free biosensors and single-cell technologies**. *Adv Colloid Interface Sci* 2022, **308**, 102727.

7. Jiang W, Liu L, Bu Y: **Application of deep learning in the phase processing of digital holographic microscopy**. *Photonics* 2025, **12**:810.

8. Liu W, Delikoyun K, Chen Q, Yildiz A, Myo SK, Sen Kuan W, *et al.*: **OAH-Net: a deep neural network for efficient and robust hologram reconstruction for off-axis digital holographic microscopy**. *Biomed Opt Express* 2025, **16**:894–909.

9. * Chen H-Y, He Y, Wang X-Y, Ye M-J, Chen C, Qian R-C, *et al.*: **Deep learning-assisted surface-enhanced Raman spectroscopy detection of intracellular reactive oxygen species**. *Talanta* 2025, **284**, 127222.
This work applies deep learning to the analysis of SERS spectra for intercellular reactive oxygen species (ROS) detection. AuNP/4-MPBA/2-MP nanoprobes are used to generate ROS-response spectra for $ONOO^-$ AND ClO^-. The collected spectra is analyzed using a two-component neural network pipeline. First a feature extractor is used to recover analyte-related SERS spectral information from background. Afterwards second 1D-CNN performs concentration prediction.

10. Zaki JK, Tomasik J, McCune JA, Bahn S, Lió P, Scherman OA: **Explainable deep learning framework for SERS bioquantification**. *ACS Sens* 2025, **10**:6597–6606.

11. Mahmud S, Sayem FR, Hassan M, Yang Y, Chowdhury MEH, Zughaier SM, *et al.*: **Deep learning-based cross-device standardization of surface-enhanced Raman spectroscopy for enhanced bacterial recognition**. *Spectrochim Acta Mol Biomol Spectrosc* 2026, **347**, 126931.

12. Wang X, Wei L, Li F, Hu Z, Fan M: **Data fusion enhanced high-dimensional SERS fingerprints construction via dual-wavelength and multisubstrate strategy for precise wastewater identification**. *Anal Chem* 2025, **97**:13551–13560.

13. * Aalizadeh M, Raut C, Afshar MA, Tabartehfarahani A, Fan X: **Accuracy enhancement in refractive index sensing via full-spectrum machine learning modeling**. *Biosensors (Basel)* 2025, **15**:582.
This work uses full-spectrum machine learning framework for refractive-index sensing. Here, the input is not manually selected peak wavelength, but simulated absorption spectrum of titanium- or silicon-based meta-grating sensors under TE and TM polarization. The pipeline applies full spectrum principal component analysis for dimensionality reduction, then applies linear regression to predict refractive-index changes.

14. Fasseaux H, Loyez M, Caucheteur C: **Machine learning unveils surface refractive index dynamics in comb-like plasmonic optical fiber biosensors**. *Commun Eng* 2024, **3**:34.

15. Cho SJ, Satasiya AD, Tamilselvan VP, Perumal AS, Solana G, Dvn Jr, *et al.*: **Protein adsorption on solid surfaces: data mining, database, molecular surface-derived properties, and semiempirical relationships**. *ACS Appl Mater Interfaces* 2024, **16**:28290–28306.

16. Šuštaršič T, Gribova V, Nikolic M, Lavalle P, Filipovic N, Vrana NE: **The effect of machine learning algorithms on the prediction of layer-by-layer coating properties**. *ACS Omega* 2023, **8**:4677–4686.

17. ** Beres B, Kovacs KD, Kanyo N, Peter B, Szekacs I, Horvath R: **Label-free single-cell cancer classification from the spatial distribution of adhesion contact kinetics**. *ACS Sens* 2024, **9**:5815–5827.
Our paper demonstrates label-free single-cell cancer classification from spatial RWG adhesion-contact kinetics. Its main importance is that high-resolution adhesion maps are linked to cell-state inference, showing that near-surface biosensor readouts can capture biomechanically informative heterogeneity at the single-cell level. It combines RWG-based data with phase-contrast microscope images to provide highly accurate single-cell localization and segmentation in lower resolution environments. After data registrations exported single-cell adhesion contact maps are passed through deep learning-based classifiers for cell-type prediction. The combination illustrates well the reference-based calibration of biosensor segmentation, which

can be extended with deep learning-based segmentation model to leave out microscopy imaging in the inferential phase.

18. Zeng T, Zhu Y, Lam EY: **Deep learning for digital holography: a review**. *Opt Express* 2021, **29**:40572–40593.

19. Bujagouni KG, Pradhan S: **DL-DHM: a novel approach for out of distribution datasets in deep learning based off-axis digital holographic microscopy**. *Opt Laser Technol* 2025, **192**, 113813.

20. Lin Z, Jia S, Xu Y, Wen B, Zhang H, Wang L, *et al.*: **Fast phase distortion identification and automatic distortion compensated reconstruction for digital holographic microscopy using deep learning**. *Opt Laser Eng* 2025, **185**, 108718.

21. * Galande AS, Thapa V, Vijay A, John R: **High-resolution lensless holographic microscopy using a physics-aware deep network**. *J Biomed Opt* 2024, **29**, 106502.
This study introduces a physics-aware deep network for high-resolution lensless holographic microscopy. The input is a single low-resolution hologram, and the proposed HDPhysnet framework combines a trained high-definition GAN with a physics-aware reconstruction network. Applied HDGAN generates high-resolution phased estimates which are applied to regularize the physics-aware network's reconstruction. It is especially relevant because the reconstruction model is constrained by physical structure, improving DHM image quality while retaining a more interpretable pipeline than purely black-box enhancement.

22. Moon I, Javidi B: **AI-driven digital holographic microscopy for label-free quantitative cellular analysis: toward low-cost and field-deployable platforms**. *Biomed Opt Express* 2026, **17**:2349–2370.

23. Yan C: **A review on spectral data preprocessing techniques for machine learning and quantitative analysis**. *iScience* 2025, **28**, 112759.

24. Coca-Lopez N: **An intuitive approach for spike removal in raman spectra based on peaks' prominence and width**. *Anal Chim Acta* 2024, **1295**, 342312.

25. Saftics A, Kurunczi S, Peter B, Szekacs I, Ramsden JJ, Horvath R: **Data evaluation for surface-sensitive label-free methods to obtain real-time kinetic and structural information of thin films: a practical review with related software packages**. *Adv Colloid Interface Sci* 2021, **294**, 102431.

26. Cuche E, Marquet P, Depeursinge C: **Spatial filtering for zero-order and twin-image elimination in digital off-axis holography**. *Appl Opt* 2000, **39**:4070–4075.

27. Otsu N: **A threshold selection method from gray-level histograms**. *IEEE Trans Syst Man Cybern* 1979, **9**:62–66.

28. Lussier F, Missirlis D, Spatz JP, Masson J-F: **Machine-learning-driven surface-enhanced raman scattering optophysiology reveals multiplexed metabolite gradients near cells**. *ACS Nano* 2019, **13**:1403–1411.

29. Chisanga M, Masson J-F: **Machine learning-driven SERS nanoendoscopy and optophysiology**. *Annu Rev Anal Chem* 2024, **17**:313–338.

30. Kovacs KD, Beres B, Kanyo N, Szabó B, Peter B, Bősze S, *et al.*: **Single-cell classification based on label-free high-resolution optical data of cell adhesion kinetics**. *Sci Rep* 2024, **14**, 11231.

31. Sztilkovics M, Gerecsei T, Peter B, Saftics A, Kurunczi S, Szekacs I, *et al.*: **Single-cell adhesion force kinetics of cell populations from combined label-free optical biosensor and robotic fluidic force microscopy**. *Sci Rep* 2020, **10**:61.

32. Matthews SA, Coelho C, Rodriguez Salas EE, Brock EE, Hodge VJ, Walker JA, *et al.*: **Real-time 3D tracking of swimming microbes using digital holographic microscopy and deep learning**. *PLoS One* 2024, **19**, e0301182.

33. Ciaparrone G, Pirone D, Fiore P, Xin L, Xiao W, Li X, *et al.*: **Label-free cell classification in holographic flow cytometry through an unbiased learning strategy**. *Lab Chip* 2024, **24**:924–932.

34. Li Y, Xiao W, Zhang H, Li X, Pan F: **Label-free detection of ovarian cancer cells in ascites-related cell models using digital holographic flow cytometry**. *Biomed Opt Express* 2026, **17**:1911–1927.

35. Nagy ÁG, Székács I, Bonyár A, Horváth R: **Simple and automatic monitoring of cancer cell invasion into an epithelial monolayer using label-free holographic microscopy**. *Sci Rep* 2022, **12**, 10111.

36. McReynolds N, Cooke FG, Chen M, Powis SJ, Dholakia K: **Multimodal discrimination of immune cells using a combination of raman spectroscopy and digital holographic microscopy**. *Sci Rep* 2017, **7**, 43631.

37. Wu Z, Feng Y, Bi R, Liu Z, Niu Y, Jin Y, *et al.*: **Image-based evaluation of single-cell mechanics using deep learning**. *Cell Regen* 2025, **14**:21.

38. ** Park S, Lee J, Park J, Moon I: **HoloFluoNet: live cell imaging intelligence based on fused holography and fluorescence for virtual staining, cell segmentation, classification, and viability analysis**. *Eng Appl Artif Intell* 2025, **161**, 112323.
This paper uses holography with fluorescence supervision for virtual staining, segmentation, classification, and viability analysis. It is especially relevant as a reference-based calibration strategy, because the auxiliary fluorescence modality teaches a biologically meaningful representation improving the segmentation performance in more complex experimental environments.

39. Malinick AS, Stuart DD, Lambert AS, Cheng Q: **Surface plasmon resonance imaging (SPRi) in combination with machine learning for microarray analysis of multiple sclerosis biomarkers in whole serum**. *Biosens Bioelectron X* 2022, **10**, 100127.

40. Jeanmaire DL, Duyne RP Van: **Surface Raman spectroelectrochemistry: part I. Heterocyclic, aromatic, and aliphatic amines adsorbed on the anodized silver electrode**. *J Electroanal Chem Interfacial Electrochem* 1977, **84**:1–20.

41. Albrecht MG, Creighton JA: **Anomalously intense Raman spectra of pyridine at a silver electrode**. *J Am Chem Soc* 1977, **99**:5215–5217.

42. Lu Y, Lin L, Ye J: **Human metabolite detection by surface-enhanced Raman spectroscopy**. *Mater Today Bio* 2022, **13**, 100205.

43. Ding Y, Sun Y, Liu C, Jiang Q-Y, Chen F, Cao Y: **SERS-based biosensors combined with machine learning for medical application**. *ChemistryOpen* 2023, **12**, e202200192.

44. Khondakar KR, Mazumdar H, Das S, Kaushik A: **Machine learning (ML)-assisted surface-enhanced raman spectroscopy (SERS) technologies for sustainable health**. *Adv Colloid Interface Sci* 2025, **344**, 103594.

45. Zambelli T, Guillaume-Gentil O, Sarajlic E, Papastavrou G, Horváth R, Liu G, *et al.*: **Fluidic force microscopy**. *Nat Rev Methods Primers* 2026, **6**:15.

46. Nagy ÁG, Kanyó N, Vörös A, Székács I, Bonyár A, Horváth R: **Population distributions of single-cell adhesion parameters during the cell cycle from high-throughput robotic fluidic force microscopy**. *Sci Rep* 2022, **12**:7747.

47. Ungai-Salánki R, Haty E, Gerecsei T, Francz B, Béres B, Sztilkovics M, *et al.*: **Single-cell adhesion strength and contact density drops in the M phase of cancer cells**. *Sci Rep* 2021, **11**, 18500.

48. Kanyo N, Kovacs KD, Saftics A, Szekacs I, Peter B, Santa-Maria AR, *et al.*: **Glycocalyx regulates the strength and kinetics of cancer cell adhesion revealed by biophysical models based on high resolution label-free optical data**. *Sci Rep* 2020, **10**, 22422.

49. Péter B, Ausbüttel T, Kanyó N, Joó P, Tóth K, Szittner Z, *et al.*: **In situ monitoring of cell adhesion kinetics using label-free optical biosensors: evaluating anticancer potential and selectivity of natural compounds**. *View* 2025, **7**, 20250061.

50. Chen B, Yin Z, Ng BW-L, Wang DM, Tuan RS, Bise R, *et al.*: **Label-free live cell recognition and tracking for biological discoveries and translational applications**. *npj Imaging* 2024, **2**:41.

51. Stokes CL, Lauffenburger DA, Williams SK: **Migration of individual microvessel endothelial cells: stochastic model and parameter measurement**. *J Cell Sci* 1991, **99**:419–430.

52. Selmeczi D, Mosler S, Hagedorn PH, Larsen NB, Flyvbjerg H: **Cell motility as persistent random motion: theories from experiments**. *Biophys J* 2005, **89**:912–931.

53. Sedaghat Z, Courbon B, Botrel H, Dugua H, Tulinski P, Alibaud L, *et al*.: **HoloMoA: a holography and deep learning tool for the identification of antimicrobial mechanisms of action and the detection of novel MoA**. *Front Microbiol* 2025, **16**, 1640252.

54. ** Bresci A, Kobayashi-Kirschvink KJ, Cerullo G, Vanna R, So PTC, Polli D, *et al*.: **Label-free morpho-molecular phenotyping of living cancer cells by combined Raman spectroscopy and phase tomography**. *Commun Biol* 2024, **7**:785.
This work combines Raman spectroscopy with phase tomography to derive live-cell morpho-molecular phenotypes. Raman maps provide molecular fingerprint and phase tomography, quantitative morphological and refractive-index-derived descriptors. Data integration strategy is applied for chemical and structural label-free modalities to create a joint feature space for phenotype discrimination.

55. Kretschmann E, Raether H: **Notizen: radiative decay of non radiative surface plasmons excited by light**. *Z Naturforsch* 1968, **23**:2135–2136.

56. Li H, Matsunaga D, Matsui TS, Aosaki H, Kinoshita G, Inoue K, *et al*.: **Wrinkle force microscopy: a machine learning based approach to predict cell mechanics from images**. *Commun Biol* 2022, **5**:361.

57. Islam K, Paul R, Wang S, Zhao Y, Adhikary P, Li Q, *et al*.: **MIML: multiplex image machine learning for high precision cell classification via mechanical traits within microfluidic systems**. *Microsyst Nanoeng* 2025, **11**:43.

58. Schmitt MS, Colen J, Sala S, Devany J, Seetharaman S, Caillier A, *et al*.: **Machine learning interpretable models of cell mechanics from protein images**. *Cell* 2024, **187**:481–494.e24.

59. Cunha I, Latron E, Bauer S, Sage D, Griffié J: **Machine learning in microscopy - insights, opportunities and challenges**. *J Cell Sci* 2024, **137**:jcs262095.

60. Adebayo J, Gilmer J, Muelly M, Goodfellow I, Hardt M, Kim B: **Sanity checks for saliency maps**. In *Proceedings of the 32nd international conference on neural information processing systems*. Curran Associates Inc.; 2018:9525–9536.

61. Ahlquist KD, Sugden LA, Ramachandran S: **Enabling interpretable machine learning for biological data with reliability scores**. *PLoS Comput Biol* 2023, **19**, e1011175.

62. Chen V, Yang M, Cui W, Kim JS, Talwalkar A, Ma J: **Applying interpretable machine learning in computational biology—pitfalls, recommendations and opportunities for new developments**. *Nat Methods* 2024, **21**:1454–1461.

63. Rudin C: **Stop explaining black box machine learning models for high stakes decisions and use interpretable models instead**. *Nat Mach Intell* 2019, **1**:206–215.